Optimal squeezing of molecular wave packets

Ilya Averbukh and Moshe Shapiro

Department of Chemical Physics, Weizmann Institute of Science, Rehovot, 76100 Israel

(Received 3 February 1993)

We present a practical method of designing laser fields for generation of spatially squeezed molecular wave packets. Our approach, based on optimal control theory, generalizes and improves previous, more intuitive suggestions for the optical generation of squeezed wave packets. Spatial-temporal evolution of the squeezing is studied and several underlying physical mechanisms of the effect are explored. Possible applications to laser femtosecond chemistry and experiments on laser modification of molecular adiabatic potentials are discussed.

PACS number(s): 42.50.Dv, 33.80.−b

I. INTRODUCTION

Recently, much interest has been devoted to the production of squeezed quantum states, i.e., states in which the noise in one observable is less than that of the vacuum state. The majority of these studies have focused on the production of squeezed radiation states [1]. A lesser amount of work was devoted to the squeezing of other (e.g., material) quantum systems [2–4].

In molecular physics, it was pointed out in the past [5,6] that squeezed wave packets may be generated by ultrashort laser pulses resonant to electronic transitions which are accompanied by a large change in the oscillator frequencies of the molecule. In addition, even pulses of *finite* duration (transform limited [7] and chirped [8]) have been shown to give rise to squeezed molecular wave packets. In contrast to $\delta(t)$-type pulses, which excite a replica of the ground-state wave function, realistic pulses generate (coherent) superpositions of such replicas. This superposition may result in a more extended or more squeezed state [7,9,10]. The mechanism underlying the production of squeezed states, in preference to extended ones, is one of the main topics to be investigated here.

Squeezing of molecular wave packets has some important applications. New developments in the technology of producing short laser pulses has made it possible to use wave packets for investigating intra-atomic and intramolecular processes in "real time" (see, e.g., [11–13]). Most of such time-resolved experiments utilize a "pump-probe" scheme, where one ("pump") laser pulse creates a wave packet on an excited electronic state and the other ("probe") pulse is used for dissociation or further excitation of the packet after an appropriate delay. In this way the hope is that excited-state dynamics can be followed in "real time" and the underlying potential "mapped."

The ability to map potential surfaces using such techniques depends, however, on the generation of highly localized wave packets by the pump source. Otherwise, the one-to-one correspondence between the delay time between pulses and the extension in coordinate space is lost [14]. Naturally, our ability to localize wave packets is limited by quantum-mechanical constraints. In addition, practical limitations restrict the type and duration of pulses used. Even if $\delta(t)$ pulses could be used, it is not clear that the shorter the pulse, the better. In fact, as noted above, the localization resulting from the use of a $\delta(t)$-type pulse is at most that of the initial (ground) state. It is of interest, therefore, to see which pulses of *finite* duration can in fact do better than a $\delta(t)$ pulse, and produce localization *exceeding* that of the ground ("vacuum") state.

This work presents a systematic study of the type of pulses capable of spatial squeezing. In order to achieve this objective, we make use of optimal control theory (OCT), an approach used in the past to design laser fields for manipulation of vibrational populations and reaction product yields [15–21]. In this first application of OCT technology to the squeezing problem, we indeed find a much greater degree of (theoretical) squeezing than that of previous studies [7–10].

The organization of this paper is as follows: Section II contains the detailed description of the optimization procedure. An illustrative example of a model, consisting of two shifted harmonic potentials, is presented in Sec. III. The results of application of the control formalism to the model are given in Sec. IV and Sec. V contains a brief discussion.

II. OPTIMIZATION PROCEDURE

We consider the excitation of a molecule, being in its ground state $|g\rangle$ at $t=0$, to a set of vibrational levels $|n\rangle$ of an excited electronic state by means of a weak laser pulse:

$$\mathcal{E}(t)=f(t)\exp(-i\Omega t)+\text{c.c.} , \tag{1}$$

where c.c. stands for complex conjugate. Here, Ω is a carrier frequency of the pulse and $f(t)$ is the pulse envelope which we allow to be a complex function of time. The dynamics of the system will be analyzed over a finite time interval $0 \le t \le T$, where T is a free parameter of our theory.

The wave function of the excited state may be expanded as

$$|\Psi(t)\rangle =\sum_{n} C_{n}(t)|n\rangle\exp(-iE_{n}t) , \tag{2}$$

where E_n is the energy of the nth state and $\hbar = 1$ throughout. The weak-field assumption enables us to express the $C_n(t)$ coefficients, using first-order perturbation theory, as

$$C_n(t) = -i\mu\langle n|g\rangle \int_0^t dt' f(t')\exp(-i\Delta_n t') ,$$

$$\Delta_n = \Omega + E_g - E_n , \qquad (3)$$

where $\langle n|g\rangle$ is an overlap ("Franck-Condon" or "form") factor and μ is an average transition dipole moment.

Our objective is to find a pulse which produces, at the end of the optimization interval T, as high a localization in coordinate space as possible. Since the shape of the final wave packet does not depend on its normalization, we fix the latter to be

$$\sum_n |C_n(T)|^2 = 1 \qquad (4)$$

and seek to minimize $\mathcal{D}$, the mean-square deviation of the wave packet about an average value $\bar{x}(T)$, given as

$$\mathcal{D} = \overline{x^2}(T) - \bar{x}^2(T) . \qquad (5)$$

Using Eqs. (2) and (4), we have that

$$\overline{x^2}(T) = \sum_{n',n} S_{n'}^*(T)(\hat{x}^2)_{n'n} S_n(T) \qquad (6)$$

and

$$\bar{x}(T) = \sum_{n',n} S_{n'}^*(T)(\hat{x})_{n'n} S_n(T) , \qquad (7)$$

where $\hat{x}$ is the position operator and

$$S_n(T) \equiv C_n(T)\exp(-iE_n T) . \qquad (8)$$

The minimization of $\mathcal{D}$ is constrained by our desire to limit the pulse bandwidth and obtain as simple a pulse as possible. We therefore introduce the following objective functional:

$$J_0[f(t),f^*(t)] = \overline{x^2}(T) - \bar{x}^2(T) + w\int_0^T dt|f(t)|^2 , \qquad (9)$$

which is to be minimized. The last term in Eq. (9) is a cost functional that has to restrict the bandwidth of $f(t)$. The value of the positive weight factor w determines the relative importance of this restriction. This is not, of course, the only possible form for the cost functional (see, e.g., the discussion in [17–21]). The heuristic background for the chosen one is the following: The more localized wave packet we are going to create, the more vibrational states lying at the wings of the absorbtion band have to be excited. This leads to the increase of the cost functional in Eq. (9), which is proportional to the energy fluence of the field. We expect that for $w \to 0$, an arbitrary small value of $\mathcal{D}$ may be achieved at the expense of obtaining a very complex looking pulse. In the opposite limit, $w \to \infty$, only very smooth pulses, producing a much smaller degree of squeezing, will result.

Due to the $\bar{x}^2(T)$ term in Eq. (9), the $J_0[f(t),f^*(t)]$ functional is highly nonlinear. To simplify the problem, we solve it in two stages. We first minimize $J_0[f(t),f^*(t)]$ while keeping $\bar{x}(T)$ fixed. Taking into ac-

count also the normalization condition Eq. (4), we introduce two Lagrange multipliers λ,λ_1 that lift both the constraints, and look for the extremal functions of another functional:

$$J[f(t),f^*(t)] = \overline{x^2}(T) - \lambda_1\bar{x}(T) - \lambda\sum_n |C_n(T)|^2$$
$$+ w\int_0^T dt|f(t)|^2 . \qquad (10)$$

Having found that one extremal function of $J[f(t),f^*(t)]$, which minimizes J_0 for a given λ_1 parameter, we next look for λ_1 yields for the desired $\bar{x}(T)$ value. While doing so, we obtain minimal values of $J_0[f(t),f^*(t)]$ corresponding to a wide range of $\bar{x}(T)$. As a byproduct, we obtain the average value of the coordinate which yields the *global* minimum of J_0. The advantage of the two-step procedure is that in contrast to J_0, the $J[f(t),f^*(t)]$ functional is quadratic and can be optimized by linear matrix methods.

Taking a functional derivative of J with respect to $f^*(t)$ and using Eqs. (3), (6), and (7), we obtain that

$$0 = \frac{\delta J}{\delta f^*(t)}$$
$$= i\mu\sum_{n',n} \langle g|n'\rangle\exp(i\Delta_{n'}t)$$
$$\times \exp(iE_{n'}T)\langle n'|\hat{x}^2 - \lambda_1\hat{x} - \lambda\hat{I}|n\rangle$$
$$\times \exp(-iE_n T)C_n(T) + wf(t) , \qquad (11)$$

where $\hat{I}$ is the unit operator. As a result, the local optimal field [i.e., the field for a certain $\bar{x}(T)$] is given as

$$f(t) = -\frac{i\mu}{w}\sum_{n',n} \langle g|n'\rangle\exp(i\Delta_{n'}t)\tilde{M}_{n'n}C_n(T) , \qquad (12)$$

where

$$\tilde{M}_{n'n} = \exp(iE_{n'}T)M_{n'n}\exp(-iE_n T) , \qquad (13)$$

$$M_{n'n} = (\hat{x}^2)_{n'n} - \lambda_1(\hat{x})_{n'n} - \lambda\delta_{n'n} . \qquad (14)$$

By inserting Eq. (12) into Eq. (3), we obtain that

$$C_k(T) = -\frac{1}{w}\sum_{n',n} P_{kn'}\tilde{M}_{n'n}C_n(T) , \qquad (15)$$

where the $P_{kn'}$ matrix is determined by the properties of the molecular absorption band

$$P_{kn} = \mu^2\langle k|g\rangle \frac{e^{i(\Delta_n-\Delta_k)T}-1}{i(\Delta_n-\Delta_k)}\langle g|n\rangle . \qquad (16)$$

Equation (15) may be presented in the form of an eigenvalue problem:

$$\sum_n Q_{kn}S_n(T) = \lambda S_k(T) , \qquad (17)$$

where the Q matrix is defined as

$$Q_{kn} = (\hat{x}^2)_{kn} - \lambda_1(\hat{x})_{kn} + w(\tilde{P}^{-1})_{kn} \qquad (18)$$

and $\tilde{P}$ as

$$\tilde{P}_{kn} = \exp(-iE_k T)P_{kn}\exp(iE_n T) . \qquad (19)$$

Of all of the eigenvalues of Q (they all render J stationary), there is one that minimizes the J_0 functional. This λ value, and the S_n vector corresponding to it, are functions of λ_1, which, as explained above, is to be determined in the second stage of optimization.

Using Eq. (12), it is possible to simplify the expression for the locally optimal J_0 functional. For the locally optimal field, we can rewrite the cost functional of Eq. (9) as

$$
w \int_0^T dt\, f^*(t) f(t)
$$

$$
= \frac{\mu^2}{w} \sum_{n',n,k,l} \langle g|n'\rangle \frac{e^{i(\Delta_{n'}-\Delta_k)T}-1}{i(\Delta_{n'}-\Delta_k)}
$$

$$
\times \langle k|g\rangle \widetilde{M}_{n'n} C_n(T) \widetilde{M}^*_{kl} C_l^*(T) . \qquad (20)
$$

It follows from Eq. (15) that

$$
w \int_0^T dt\, f^*(t) f(t) = -\sum_{k,l} C_k(T) \widetilde{M}^*_{kl} C_l^*(T)
$$

$$
= -\sum_{k,l} S_l^*(T) M_{lk} S_k(T) , \qquad (21)
$$

and by substituting Eq. (14) for the M matrix into Eq. (21), we obtain that

$$
J_0^{\mathrm{opt}}(\lambda_1) = \lambda_1 \bar{x}(\lambda_1) + \lambda(\lambda_1) - [\bar{x}(\lambda_1)]^2 . \qquad (22)
$$

In the final stage of optimization, we adjust the λ_1 parameter to satisfy the requirement that

$$
\bar{x}(\lambda_1) = \sum_{n',n} S_{n'}^*(T,\lambda_1)(\hat{x})_{n'n} S_n(T,\lambda_1) = \bar{x} . \qquad (23)
$$

Alternatively, if we lift the constraint that the wave packet is to be centered at $x = \bar{x}$, we can vary λ_1 to find the *global* minimum of J_0. This yields the highest degree of squeezing possible for the given molecular model. Both of these nonlinear [but one-dimensional (1D) problems] may be solved by means of simple iterative procedures.

III. APPLICATION TO PARABOLIC POTENTIALS

To test the proposed procedure, we have investigated the excitation of a model molecular system composed of two displaced harmonic potentials. The Franck-Condon factors for transitions from the ground level of the lower state whose frequency is ω_1 to the nth vibrational level of the upper state (with frequency ω_2) are given by the well-known expression [22,23]

$$
\langle n|g\rangle = \left[\frac{4s}{(s+1)^2} \right]^{1/4} \left[\frac{s-1}{s+1} \right]^{n/2}
$$

$$
\times \frac{1}{\sqrt{2^n n!}} H_n \left[\frac{\sqrt{2}s}{(s^2-1)^{1/2}} \alpha \right]
$$

$$
\times \exp\left[-\frac{2s}{s+1}\alpha^2 \right] , \qquad (24)
$$

where

$$
s = \frac{\omega_1}{\omega_2}, \quad \alpha = x_s \left[\frac{m\omega_2}{2\hbar} \right]^{1/2} . \qquad (25)
$$

Here, x_s is the shift between the equilibrium positions of the two oscillators, m is the reduced mass, and $H_n(z)$ are the Hermite polynomials. We note that in the equal frequencies case ($\omega_1 = \omega_2 = \omega$), the wave function of the ground state is a coherent state $|\alpha\rangle$ of the upper harmonic potential. The Franck-Condon factors are then reduced to

$$
\langle n|\alpha\rangle = e^{-\alpha^2/2} \frac{\alpha^n}{\sqrt{n!}} . \qquad (26)
$$

For $\alpha \geq 1$, the Gaussian approximation for (26),

$$
\langle n|\alpha\rangle^2 \approx \frac{1}{\sqrt{2\pi\bar{n}}} \exp\left[-\frac{(n-\bar{n})^2}{2\bar{n}} \right], \quad \bar{n} = \alpha^2 \qquad (27)
$$

may be used very well. Considerable simplifications ensue if T (the time at which maximal squeezing is to occur) is chosen to be a multiple of the vibration period ($T = 2\pi l/\omega_2$; l is an integer). In this case the P matrix of Eq. (16) takes the diagonal form

$$
P_{kn} = \mu^2 \langle k|g\rangle^2 T \delta_{kn} , \qquad (28)
$$

and the pulse shape (12) is given by the simple expression

$$
f(t) = \frac{i}{\mu T} \sum_n e^{i\Delta_n t} \frac{C_n(T)}{\langle n|g\rangle} . \qquad (29)
$$

In deriving Eq. (29), we have used the relationship

$$
\sum_n M_{n'n} C_n(T) = -w \sum_n (P^{-1})_{n'n} C_n(T) , \qquad (30)
$$

which follows from Eq. (15). Finally, the necessary matrix elements for the coordinate operator are obtained by the usual expressions for a harmonic oscillator [24]:

$$
x_{nk} = \left[\frac{n}{2} \right]^{1/2} \delta_{n-1,k} + \left[\frac{n+1}{2} \right]^{1/2} \delta_{n+1,k} , \qquad (31)
$$

$$
x_{nk}^2 = \frac{1}{2}\sqrt{n(n-1)}\delta_{n-2,k} + (n+\tfrac{1}{2})\delta_{nk}
$$

$$
+ \frac{1}{2}\sqrt{(n+1)(n+2)}\delta_{n+2,k} . \qquad (32)
$$

Here and below, the coordinate is measured in the units of $\sqrt{\hbar/m\omega_2}$.

IV. RESULTS

Calculations were done for several values of the shift parameter α and frequency ratio s that control the shape of the molecular absorption band. In each case the carrier frequency of the pulse Ω was chosen to be in resonance with the "vertical" transition frequency (from the ground state to the $n = \alpha^2$ level). The oscillator basis set was truncated at some $n = N_{\max}$, depending on the parameters of the model and optimization procedure. At each step of the optimization process, convergence to within 1% in the values of the expansion coefficients $|C_n|^2$ was attained.

We present results obtained for the case of $|\alpha| = 3$ and

for equal frequencies $(\omega_1 = \omega_2 = \omega)$. Below, all the variables are reduced to dimensionless form. The unit of time is equal to the vibrational period $2\pi/\omega$, f is measured in the units of $\hbar\omega/(2\pi\mu)$, and the unit of w is $2\pi\mu^2/(\hbar m \omega^2)$.

Excitation by nonoptimized ultrashort laser pulse creates a replica of the ground-state wave function in the excited potential, which results in a Gaussian wave packet with a coordinate mean-square deviation of $\mathcal{D}=0.5$. This wave packet oscillates between the $x \approx \pm 4.2$ classical turning points.

Figure 1 presents the numerical results when optimization is performed. Shown is the locally optimal J_0^{opt} value [see Eq. (22)] as a function of λ_1 for $w=0.01$ and $T=1$ [Fig. 1(a)]. It is clear that J_0^{opt} is an even function of λ_1 in this case. Figure 1(b) displays the relationship between λ_1 and $\bar{x}$ for the same optimal solution. Thus, the global extremum of J_0^{opt} achieved at $\lambda_1 = 0$ corresponds to $\bar{x} = 0$.

Figure 1(b) also allows us to consider the alternative constraint in which the final squeezed wave packet has to be centered at some fixed coordinate position $\bar{x}$. Using this graph, we simply locate the λ_1 parameter corresponding to the desired $\bar{x}$ value. Figures 2(a)–2(c) display the time dependence of the optimal pulse field $f(t)$ for $\bar{x}=2$. The power spectrum of the electromagnetic field $\mathcal{E}(t)$ is shown in the Fig. 2(d). It consists of a number of
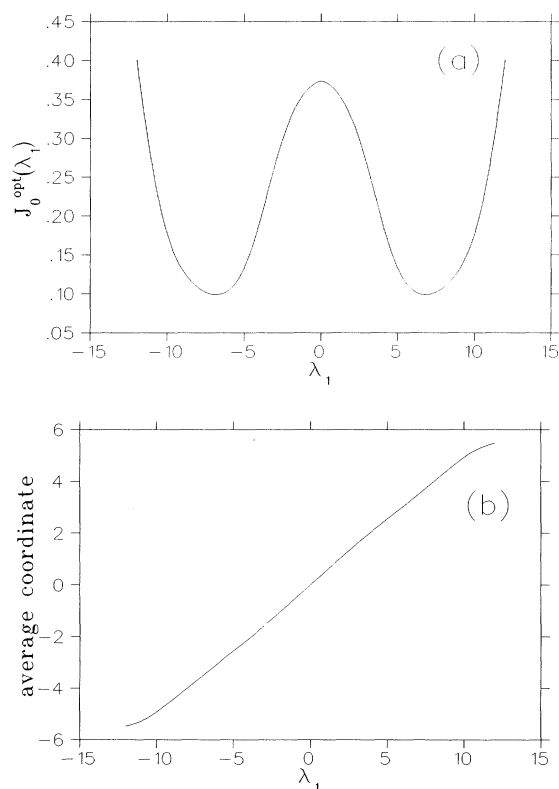
FIG. 1. Dependence of the (a) minimal value of the objective functional (9) and (b) average coordinate position $\bar{x}$ on the λ_1 Lagrange multiplier. The optimization time interval T equals the period of one vibration. $s=1$, $\alpha=-3$, and $w=0.01$.
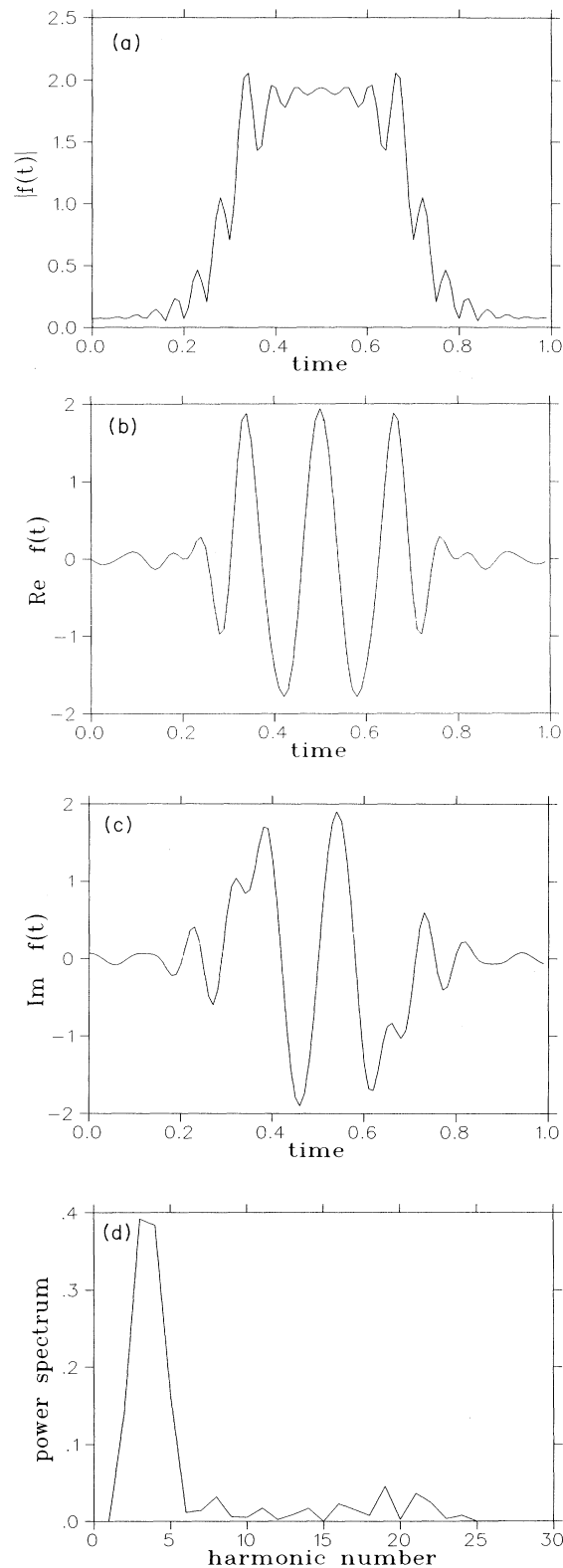
FIG. 2. Time dependence of the (a) modulus, (b) real part, and (c) imaginary part of the optimal pulse. Time is measured in the units of vibrational period. (d) Power spectrum of the field. $s=1$, $\alpha=-3$, $w=0.01$, and $\bar{x}=2$.

harmonics corresponding to the transitions to the vibrational levels of the excited state. Although our input carrier frequency was chosen to be in resonance with the transition to the $n = \alpha^2 = 9$ level, it is clear from Fig. 2(d) that the optimal "carrier frequency" (the central frequency of the optimal field) is shifted to the red with respect to the "vertical" transition.

The time evolution of the modulus squared of the corresponding wave function in the upper electronic term is shown in Figs. 3(a)–3(c). At the initial time a considerable probability density is generated near the left turning point $(x = -4.2)$. This is a result of the "vertical"
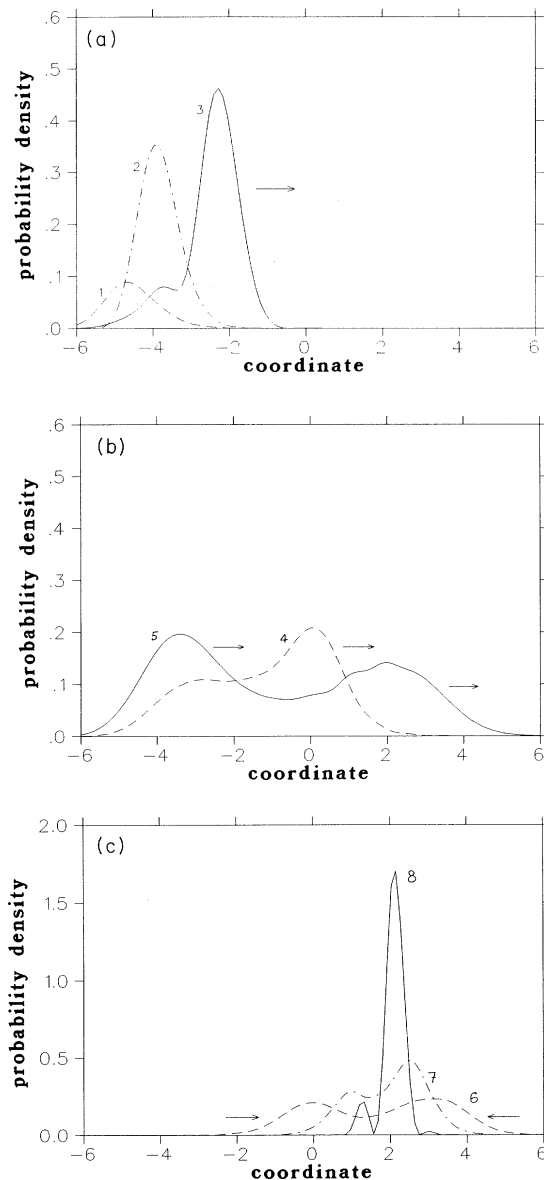
FIG. 3. Time evolution of the wave-function modulus squared: (a) $t/T = 0.35$, 0.4, and 0.5 for curves 1, 2, and 3, respectively; (b) $t/T = 0.6$ and 0.7 for curves 4 and 5, respectively; (c) $t/T = 0.9$, 0.95, and 1.0 for curves 6, 7, and 8, respectively.

pumping from the ground state. As time progresses, portions of the wave function are seen to move to the right under the action of the restoring force [see Fig. 3(a)]. As a result of a cooperative effect between the wave-packet motion and the pulse (which is still present), the wave function splits into two wavelets at about $T/2$ [Fig. 3(b)]. At a latter time the wavelet in the front is reflected from the right turning point and two wavelets begin to approach each other and merge [curves 6, 7, and 8 in Fig. 3(c)]. We see the emergence of a sharp squeezed wave packet centered near $x = 2$ [curve 8 in Fig. 3(c)]. At this instant, the mean-square deviation $\mathcal{D}$ of the wave-packet coordinate is just 0.12, i.e., considerably less the corresponding value $\mathcal{D} = 0.50$ for the ground-state wave function. The mechanism of squeezing presented here (i.e., the creation of a linear superposition of several wave packets) is similar to that investigated in several papers [7,9,10].

Figure 4 shows pulses analogous to that presented in Fig. 2, for larger values of the w parameter. Because of the discriminative role of the last term in the functional of Eq. (9), the Fourier components of the field, lying at the wings of the absorption band, become suppressed. The larger the w value, the simpler and smoother the optimal pulse. Nevertheless, the squeezing mechanism remains the same; it results from two wave packets which interfere in a given space point. Naturally, the simpler looking pulses produce broader wave packets ($\mathcal{D} = 0.3$, 0.7, and 1.8 for $w = 0.1$, 1, and 10, respectively).

According to Fig. 1(a), the global minimum of J_0^{opt} for $w = 0.01$ (and $T = 1$) is achieved at $\lambda_1 \approx \pm 6.8$, corresponding to $\bar{x} = \pm 3.4$. This means that under the imposed restrictions, the greatest degree of squeezing ($\mathcal{D} = 0.07$) is possible near the classical turning points. In Figs. 5(a) and 5(b) we present the pulse shape and the power spectrum of the field for $\lambda_1 = 6.8$ ($\bar{x} = 3.4$). Note that the pulse vanishes at the ends of the optimization interval, although it has not been imposed directly. The structure of the power spectrum is related to the well-known fact that the distribution of the energy-level population has an oscillatory behavior as a function of n for highly squeezed states [25].
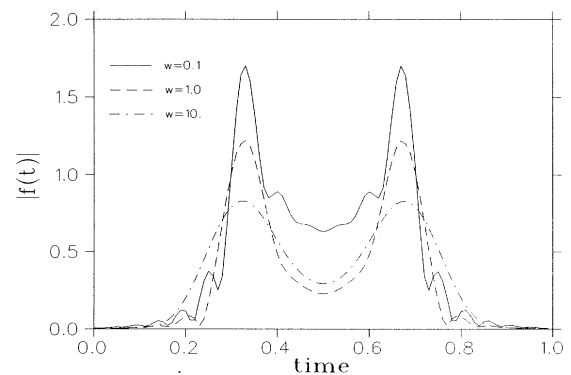
FIG. 4. Time dependence of the optimal pulse for different values of the weight factor w. Time is measured in the units of vibrational period. $s = 1$, $\alpha = -3$, and $\bar{x} = 2$.
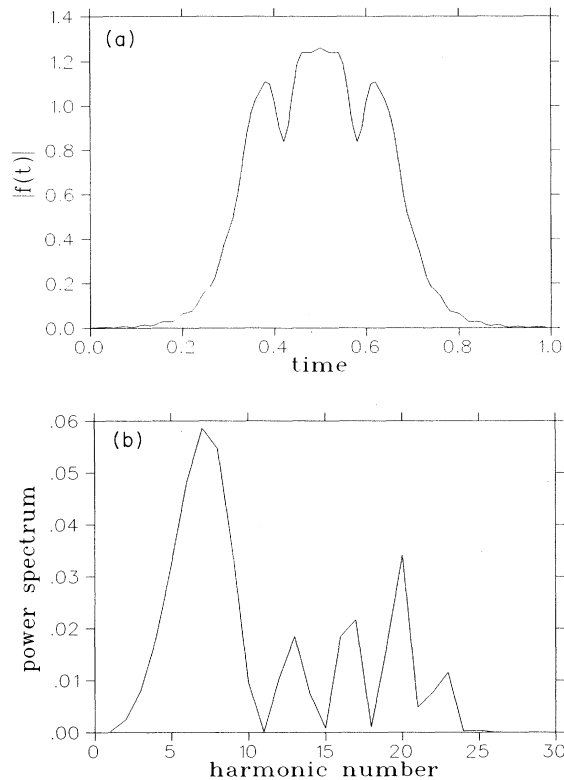
FIG. 5. (a) Time dependence and (b) power spectrum of the field providing global minimum of the objective functional (9) for $w = 0.01$ and $T = 1$ ($s = 1$, $\alpha = -3$).

The time evolution of the wave function for this case is displayed in Fig. 6. Creation of the wave packet starts again near the left turning point at $x = -4.2$. At $t/T \approx 0.75$, a much-broadened wave packet (squeezed in momentum space) appears, which is centered around the equilibrium position and is moving to the right. At this point in time the pulse is almost over, and the following dynamics is that of a free-evolving wave-packet. As this wave packet continues moving towards the right turning
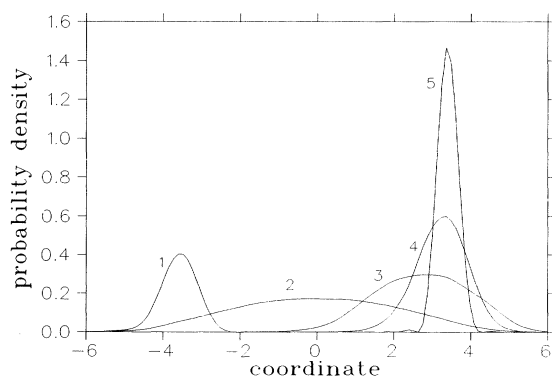
FIG. 6. Time evolution of the wave-function modulus squared for the field presented in Fig. 5. Here, $t/T = 0.5$, 0.75, 0.90, 0.95, and 1.0 for curves 1–5, respectively.
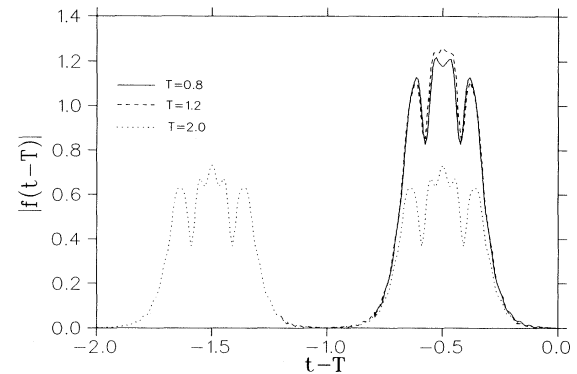
FIG. 7. Optimal pulses providing global minimum of the objective functional for different durations T of the optimization interval. $s = 1$, $\alpha = -3$, and $w = 0.01$.

point ($x = 4.2$), it becomes narrower and narrower due to the slowing down of its front. At $t/T = 1$, the reflected front meets the tail of the wave packet, resulting in the maximal squeezing shown in Fig. 6 (curve 5). Thus, in this case the squeezing is initially achieved in momentum space, and then after one-quarter of the vibrational period, in coordinate space.

To see how the value of the time interval T affects the shape of the pulse, several fields realizing a global minimum of the objective functional were calculated for the same value of w and different T (see Fig. 7). The fields are plotted as the functions of t-T. We see that for optimization intervals longer than the duration of the pulse of Fig. 5(a), the optimal field becomes almost independent of T (see the curves for $T = 0.8$ and 1.2). In each case the maximum of the optimal pulse occurs one-half of a vibrational period before the end of the interval. The optimization algorithm "knows" that the best squeezing is most easily achieved near the turning point. If, however, the length of the interval includes several vibrational periods, the algorithm "prefers" to use a periodic sequence of several pulses rather than a single one with the same form (see curve for $T = 2.0$ in Fig. 6). One can explain this effect as due to the fact that the total probability of excitation by N pulses, separated in time by a vibrational period, scales as N^2, while the energy fluence scales only as N. Therefore, the splitting of a single pulse into a periodic sequence has an advantage for minimization of the objective functional (9).

V. SUMMARY

In this work we have demonstrated how optimal control theory may be used to design optical pulses which create the "most" localized wave packet. We have introduced an objective functional for minimization of the spatial width of the wave packet while keeping a simple laser pulse shape. This is achieved via a "cost" function that restricts the bandwidth of the laser, and happens to be proportional to the energy fluence of the pulse. A free weight factor balances the degree of squeezing against the complexity of the field.

We have suggested a two-step numerical algorithm which reduces the nonlinear optimization procedure to the solution of an eigenvalue problem. The formalism was tested using a simple model of a molecule with two electronic states described by two displaced harmonic potential curves. The designed optimal fields generate wave packets which are much more localized than the ground-state vibrational wave function. In some cases our procedure reproduces the previous "intuitive guesses" as to the choice of pulse shapes leading to squeezing. Thus, the mechanism of generating a strongly localized nuclear wave function as a result of interference of two wavelets in the vicinity of a classical turning point [10] comes out automatically in the present scheme. In general, however, the squeezing is attained by a complex cooperative interplay of the intramolecular coherence and the pumping field, whose amplitude-phase properties cannot be easily guessed.

Although the formalism has been tested here using a harmonic system, it is valid for any nonlinear molecular adiabatic potentials. An interesting future application of our procedure may be to the experiments [26,27] where intense laser fields are used to modify molecular potentials. In these experiments strong light-induced avoided crossings of electronic states result in new bound molecular states with additional equilibrium positions. To trap a molecule in these states, a considerable portion of the wave function must be localized in the vicinity of the crossing just before the modifying laser is switched on. Our method of optimal squeezing may be implemented to this end at the initial stage of trapping. A more detailed discussion of this aspect will be published shortly.

ACKNOWLEDGMENT

[1] See, e.g., special issues on squeezing and nonclassical light, J. Opt. Soc. Am. B **4** (1987); J. Mod. Opt. **34** (6) (1987); **34** (7) (1987).

[2] X. Ma and W. Rhodes, Phys. Rev. A **39**, 1941 (1989).

[3] G. S. Agarwal and S. A. Kumar, Phys. Rev. Lett. **67**, 3665 (1991).

[4] C. F. Lo, Phys. Rev. A **43**, 404 (1991); **45**, 5262 (1992).

[5] J. Janszky and Y. Y. Yushin, Opt. Commun. **59**, 151 (1986).

[6] R. Graham, J. Mod. Opt. **34**, 873 (1987).

[7] J. Janszky and An. V. Vinogradov, Phys. Rev. Lett. **64**, 2771 (1990).

[8] J. Janszky, T. Kobayashi, and An. V. Vinogradov, Opt. Commun. **76**, 30 (1990).

[9] V. Buzek and P. L. Knight, Opt. Commun. **81**, 331 (1991).

[10] W. Schleich, M. Pernigo, and Fam Le Kien, Phys. Rev. A **44**, 2172 (1991).

[11] A. H. Zewail, Science **242**, 1645 (1988); M. J. Rosker, M. Dantus, and A. H. Zewail, *ibid.* **241**, 1200 (1988).

[12] G. Alber and P. Zoller, Phys. Rep. **199**, 231 (1991).

[13] I. Sh. Averbukh and N. F. Perelman, Usp. Fiz. Nauk **161**, 41 (1991) [Sov. Phys.—Usp. **34**, 572 (1991)].

[14] J. L. Krause, M. Shapiro, and R. Bersohn, J. Chem. Phys. **94**, 5499 (1991).

[15] D. J. Tannor and S. A. Rice, J. Chem. Phys. **83**, 5013 (1985); Adv. Chem. Phys. **70**, 441 (1988).

[16] D. J. Tannor, R. Kosloff, and S. A. Rice, J. Chem. Phys. **85**, 5805 (1986).

[17] S. Shi, A. Woody, and H. Rabitz, J. Chem. Phys. **88**, 6870 (1988).

[18] A. Pierce, M. Dahleh, and H. Rabitz, Phys. Rev. A **37**, 4950 (1988).

[19] R. Kosloff, S. A. Rice, P. Gaspard, S. Tersigni, and D. J. Tannor, Chem. Phys. **139**, 201 (1989).

[20] C. D. Schweiters and H. Rabitz, Phys. Rev. A **44**, 5224 (1991).

[21] R. S. Judson and H. Rabitz, Phys. Rev. Lett. **68**, 1500 (1992).

[22] J. Katriel, J. Phys. B **3**, 1315 (1970).

[23] H. P. Yuen, Phys. Rev. A **13**, 2226 (1976).

[24] L. D. Landau and E. M. Lifshitz, *Quantum Mechanics: Non-Relativistic Theory* (Pergamon, New York, 1977).

[25] W. Schleich and J. A. Wheeler, J. Opt. Soc. Am. B **4**, 1715 (1987).

[26] A. Zavriyev, P. H. Bucksbaum, H. G. Muller, and D. W. Schumacher, Phys. Rev. A **42**, 5500 (1990).

[27] B. Yang, M. Saeed, L. F. Mauro, A. Zavriyev, and P. H. Bucksbaum, Phys. Rev. A **44**, R1458 (1991).